Investigation of the Effects of Stator Slot Permeance on Induction Motor and Obtaining the Best Starting Torque Using Permeance Calculation

Étude des effets de la perméance de la fente du stator sur les moteurs asynchrones et obtention du meilleur couple de départ à l'aide du calcul de perméance

Asım Gökhan Yetgin

***Abstract*— In induction motors, the leakage reactance values are obtained from the motor short circuit operation experiment. However, these values do not give clear results for different geometries. For this reason, taking into the parameters of the slot geometry accounts for determining the stator and rotor leakage reactance values that are important in terms of obtaining more accurate results. This paper has investigated the stator slot permeance values of nine different stator slot structures commonly used in industrial type of three-phase squirrel cage induction motors for obtaining the best starting torque. The stator inductance and leakage reactance values were calculated for each stator slot structure. The change of starting torque of the induction motor has been analyzed by using the MATLAB code. As a result of the analysis, the stator slot structure, which gives the best starting torque, has been obtained. It has been also shown that a 16% improvement can be achieved by changing the stator slot structure at the starting torque. This increase in the starting torque will provide a great advantage for the motor's acceleration versus a heavy load.**

***Résumé*— Dans les moteurs asynchrones, les valeurs de réactance de fuite sont obtenues à partir du test de fonctionnement en court-circuit du moteur. Cependant, ces valeurs ne donnent pas des résultats clairs pour différentes géométries. Par conséquent, compte tenu des paramètres de la géométrie de la fente lors de la détermination des valeurs de réactance de fuite du stator et du rotor est important pour obtenir des résultats plus précis. Cet article explore la perméabilité de rainure de stator de neuf structures de rainure de stator différentes couramment utilisées dans les moteurs à induction triphasés à cage d'écureuil de type industriel afin d'obtenir le meilleur couple de déplacement. Les valeurs d'inductance et de réactance de fuite du stator ont été calculées pour chaque structure de rainure de stator. La variation du couple de déplacement du moteur asynchrone a été analysée à l'aide du code MATLAB. À la suite de l'analyse, on a obtenu une structure de rainure de stator qui donne le meilleur couple de démarrage. Il a également été démontré qu'une amélioration de 16% pouvait être obtenue en modifiant la structure de rainure du stator au moment du déplacement. Cette augmentation du couple donnera un grand avantage contre une charge lourde dans l'accélération du moteur.**

***Index Terms*— Calculation of inductance, calculation of reactance, induction motor, permeance, starting torque.**

I. Introduction

THE greatest part of produced electrical energy is consumed by motors of industrial and commercial enterprises. Despite the great variety of motor types (direct current, electronic commutator motors, synchronous, permanent magnetic field synchronous motors, hysteresis, and stepper motors) used, induction motors are the horse of the industry [1] due to their size, low manufacturing cost, simple structure, robustness, and high reliability [2], [3]. Since the squirrel cage induction motor became the most common industrial applications, manufacturers have obtained large amounts of data on torque-slip and current-slip curves [4]. In order to obtain these curves, single-phase equivalent circuit of the induction motor has to be obtained. Three-phase induction motors under steady-state operation are commonly modeled using a per-phase equivalent circuit, which enables the calculation of quantities such as line current, power factor, input and output powers, torque values, and efficiency as a function of supply voltage, frequency, and slip. The equivalent circuit parameter

Manuscript received February 11, 2019; revised April 18, 2019; accepted May 1, 2019. Date of current version September 9, 2019.

The author is with the Department of Electrical and Electronics Engineering, Faculty of Engineering and Architecture, Burdur Mehmet Akif Ersoy University, Burdur 15030, Turkey (e-mail: agyetgin@mehmetakif.edu.tr).

Associate Editor managing this paper's review: Om Malik.

Digital Object Identifier 10.1109/CJECE.2019.2914959

values are traditionally obtained via no-load and locked-rotor tests [5]. In induction motors, the total leakage reactance value (X_k) is found with (1). In this equation, R_k is the total resistance and Z_k is the total impedance. Stator leakage reactance (X_1) and rotor leakage reactance (X_2) values are determined using (2) based on the IEC standard for single-cage and double-cage induction motors [6]. The other method to distinguish X_1 and X_2 parameters is to perform stator and rotor slot permeance calculations. By doing these calculations, stator and rotor leakage reactance values can be obtained separately

$$X_k = \sqrt{Z_k^2 - R_k^2} \tag{1}$$

$$X_1 = X_2 = \frac{X_k}{2} \text{ for single cage}$$

$$\frac{X_1}{X_2} = 0.67 \text{ for double cage.} \tag{2}$$

Bao *et al.* [7] compared the starting performances of the motor models that have got two typical stator slots and the flux leakage characteristics. They used finite-element models for different stator slot type analyses. They concluded that the slot permeance factor has a direct impact on the slot leakage reactances. Nishihama *et al.* [8] expressed that the magnetic saturation by the leakage flux cannot be ignored on the motor characteristics estimation in the high slip range, such as starting torque, since the current generates a large amount of leakage flux. Dong *et al.* [9] calculated a stator slot leakage reactance and an end winding leakage reactances of an induction motor which have a semiclosed stator slot geometry. Li *et al.* [10] presented an analytical method of evaluating slot and zig-zag leakage flux, permeance variations, and instantaneous torque in their paper. They concluded that larger stator or rotor slot opening width reduces the slot leakage, zig-zag leakage inductances, and increases the average torque. Boglietti *et al.* [11] described how to calculate the stator inductance values of single-layer and double-layer induction motors in their paper. Nandi [12] investigated the effect of rotor slot permeance values on rotor slot harmonics and used semiopen and closed rotor geometries for analysis.

There are a lot of studies on the stator and rotor slot structures of squirrel cage induction motors. However, these studies have been usually carried out as a comparison of one or two stator and rotor slots. In addition, torque–speed curves have been obtained from no-load, short circuit, and loaded operation experimental tests in these studies. In this paper, torque–speed graphs have been obtained by using stator slot permeance coefficient calculation unlike studies in the literature.

In this paper, the change of the starting torque of induction motors has been analyzed according to the stator slot permeance coefficient. Nine different stator slot geometries have been used in the analyses. The aim of this paper is to determine the geometry of the slot which will give the best starting torque using the permeance values. Moreover, the inductance and reactance changes have been analyzed for each slot structure. Also, torque–speed graphs have been obtained and interpreted. The MATLAB software has been used for permeance calculating.

II. Materials and Method

A. Slot Permeance Calculation

The inductance is determined under the knowledge of the spatial distribution of the stator magnetic flux and its Ampere-turn. However, many problems give rise to the determination of the leakage inductance of windings. In the three-phase induction machine model, the leakage flux of each winding consists of slot leakage flux, air-gap leakage flux, and end winding and skew leakage flux. The largest participation in the total leakage flux has the component associated with the slot leakage one. So far, in order to calculate the slot leakage inductance, the complex values are generally used. However, in this way, the slot leakage inductance has been determined for the steady state of an induction machine [13].

The flux in a rotating machine can be considered as useful flux and leakage flux. The useful flux provides energy conversion, while the leakage flux gives winding leakage inductance and reactance. The useful flux links the windings, on both sides of the air gap, leakage flux links with either of the windings (on the stator or the rotor) but not both. The types of permeance to be considered are as follows [14]–[17]: slot permeance (λ_s), overhang permeance (λ_{over}), zig-zag permeance (λ_{zz}), belt permeance (differential) (λ_{dif}), and skewing permeance (λ_{skew}).

The total permeance of the induction motor is obtained by the following:

$$\lambda_{total} = (\lambda_s + \lambda_{over} + \lambda_{zz} + \lambda_{dif} + \lambda_{skew}). \tag{3}$$

B. Inductance and Reactance Calculation

After calculating the total permeance values for each stator slot shape, stator inductance and reactances are separately calculated using the following:

$$L_1 = \frac{\mu_0 \cdot L \cdot T_{ph}^2}{p \cdot q} \cdot \lambda_{total} \tag{4}$$

$$X_1 = 2 \cdot \pi \cdot f \cdot L_1 \tag{5}$$

where μ_0 is the magnetic permeability coefficient, p is the number of poles, f is the frequency in hertz, T_{ph} is the number of turns per phase, q is the number of slots per-pole per-phase, L is the length of the conductor in core, and λ_s is the slot permeance coefficient [14]. Zig-zag and skewing permeance are not included in the permeance calculation because of their very small values.

C. Induction Motor Starting Characteristics

Stator and rotor slot design is one of the most critical parameters of the induction motor design process. Different structures of the slot types change resistance and reactance values of the motor. The torque–speed characteristic curves change depending on these values. The general torque formula of the induction motor is given in (6). It has been easily seen that the torque value is changing with the stator and rotor resistances and reactances, as well as the number of phase (m),

TABLE I
REFERENCE MOTOR SPECIFICATION [18]

Parameters	Values
Power	15 kW
Rotor speed	1746 rpm
Voltage	460 V
Number of pole	4
Frequency	60 Hz
Efficiency	92%
Stator current	20 A
Frame	NEMA B, 256 T
Stator slot type	ST 4 (Fig. 1. d)
Stator resistance	0.3745 ohm
Stator reduced rotor resistance	0.43 ohm
Rotor leakage reactance	1.696 ohm
Winding connection	Star
Axial length	120 mm
Number of stator turns per phase	144 turns
Number of stator slot per-pole per-phase	4

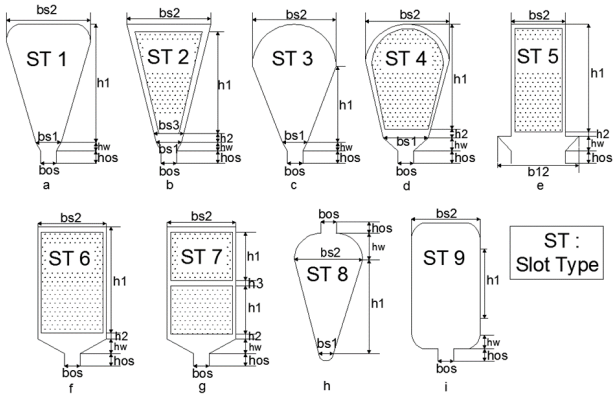

Fig. 1. Stator slot types.

the voltage (V_1), frequency, number of poles, and the slip (s)

$$T = \frac{m \cdot p}{2 \cdot \pi \cdot f} \cdot \frac{R_2}{s} \cdot \frac{V_1^2}{\left(R_1 + \frac{R_2}{s}\right)^2 + (X_1 + X_2)^2}. \quad (6)$$

In this paper, $s = 1$ has been taken to see the changes in starting torque and considering that the other parameters except the stator reactance are fixed. The variation in the starting torque has been investigated based on the stator permeance values obtained for each motor slot structure. The reference motor's parameters have been given in Table I.

III. MATH METHOD DESCRIPTION

The general stator slot structures of the induction motor have been shown in Fig. 1. Slot opening width $b_{os} = 1$ mm, slot opening height $h_{os} = 1$ mm, slot wedge height $h_w = 2$ mm, slot top width $b_{s2} = 8.88$ mm, slot bottom width $b_{s1} = 4.54$ mm, slot height $h_1 = 40.5$ mm, and $h_2 = 0.5$ mm have been standardized for the reference motor (ST4) in Fig. 1. The values of the other stator slot structure used in the motor are as following: $h_3 = 0.5$ mm, $b_{s3} = 5$ mm, and $b_{12} = 15$ mm.

The stator slot permeance formulas for each slot structure depending on the slot parameters have been given in the following [14], [15], [18]–[23]:

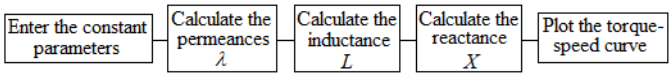

Fig. 2. MATLAB algorithm flowchart.

$$\lambda_s = \left(\frac{2 \cdot h_1}{3 \cdot (b_{s1}+b_{s2})} + \frac{2 \cdot h_w}{b_{os}+b_{s1}} + \frac{h_{os}}{b_{os}}\right)\left(\frac{1+3 \cdot \beta}{4}\right) \quad \text{(for } a\text{)}$$

$$\lambda_s = \left(\frac{2 \cdot h_1}{3 \cdot (b_{s3}+b_{s2})} + \frac{2 \cdot h_2}{b_{s1}+b_{s3}} + \frac{2 \cdot h_w}{b_{s1}+b_{os}} + \frac{h_{os}}{b_{os}}\right) \quad \text{(for } b\text{)}$$

$$\lambda_s = \mu_0 \cdot \left(\frac{h_{os}}{b_{os}} + \frac{2 \cdot h_w}{b_{s1}+bs_2} + \frac{h_1}{3 \cdot b_{s1}} \cdot k_t\right) \quad \text{(for } c\text{)}$$

$$\lambda_s = \frac{2 \cdot h_1 \cdot K_2}{3 \cdot (b_{s1}+b_{s2})} + \left(\frac{h_{os}}{b_{os}} + \frac{h_w}{bs_1} - \frac{b_{os}}{2 \cdot b_{s1}} + 0.785\right) \cdot K_1 \quad \text{(for } d\text{)}$$

$$\lambda_s = \frac{h_1}{3 \cdot b_{s2}} + \frac{h_2+h_{os}}{b_{s2}} + \frac{2 \cdot h_w}{b_{12}+b_{s2}} \quad \text{(for } e\text{)}$$

$$\lambda_s = \frac{h_1}{3 \cdot b_{s2}} + \frac{h_2}{b_{s2}} + \frac{2 \cdot h_w}{b_{s2}+b_{os}} + \frac{h_{os}}{b_{os}} \quad \text{(for } f\text{)}$$

$$\lambda_s = \frac{2 \cdot h_1}{3 \cdot b_{s2}} + \frac{h_3}{4 \cdot b_{s2}} + \frac{h_2}{b_{s2}} + \frac{h_w}{b_{s2}+b_{os}} + \frac{h_{os}}{b_{os}} \quad \text{(for } g\text{)}$$

$$\lambda_s = \frac{2 \cdot h_1 \cdot K_2}{3 \cdot (b_{s2}+b_{s1})} + \left(\frac{h_{os}}{b_{os}} + \frac{h_w}{b_{s2}} - \frac{b_{os}}{2 \cdot b_{s2}} + 0.785\right) \cdot K_1 \quad \text{(for } h\text{)}$$

$$\lambda_s = \frac{h_1}{3 \cdot b_{s2}} + \frac{h_{os}}{b_{os}} + 0.41 + 0.76 \cdot \log\left(\frac{b_{s2}}{b_{os}}\right) \quad \text{(for } i\text{)} \quad (7)$$

where t is the ratio of the width of stator slot top to the width of stator slot bottom and it has been given in (8). k_t, the constant coming from slot geometry depending on the t parameter and k_t has been given in the following:

$$t = \frac{b_{s2}}{b_{s1}} \quad (8)$$

$$k_t = 3 \cdot \frac{(4 \cdot t^2 - t^4 \cdot (3 - 4 \cdot \ln(t) - 1))}{(t^2 - 1)^2 \cdot (t - 1)}. \quad (9)$$

β is the ratio of coil pitch over pole pitch (the chording factor) and it can be calculated from (10). In the expression, y is the chorded coil and τ is the pole pitch. In this paper, τ is obtained based on the number of stator slot (N_s) and the number of pole (p). y has been chosen 11, in other words, a layer winding with chorded coil: $\tau = (N_s/2 \cdot p) = (48/2.2) = 12$ and $\beta = (11/12)$. K_1 and K_2 are the constants that change by depending on the chording factor given in (10). The formulas of these expressions have been given in (11)

$$\beta = \frac{y}{\tau} \quad (10)$$

$$K_1 = \frac{1}{4} + \frac{1}{4} \cdot \beta \quad \text{and} \quad K_2 = \frac{1}{4} + \frac{3}{4} \cdot K_1. \quad (11)$$

The MATLAB structure for calculating the stator slot permeance coefficient, inductance, and reactance values from nine different stator slot geometries has been shown in Fig. 2. First, the required parameters for slot structures have been defined. Then, the stator slot permeance coefficient, inductance, and

TABLE II
PERMEANCE, INDUCTANCE, REACTANCE, AND STARTING TORQUE RESULTS FOR NINE SLOT TYPES

Slot type [ST]	Stator slot permeance coefficient	Inductance [H]	Stator reactance [ohm]	Starting torque [N.m]
1	3.593717214	0.001738118	0.655255306	78.15
2	3.772088420	0.001772978	0.668397019	77.40
3	3.953330419	0.001808398	0.681750241	76.61
4	2.239642753	0.001473488	0.555492243	84.44
5	1.856693376	0.001398648	0.527277987	86.35
6	2.981434876	0.001618459	0.610144669	80.91
7	4.471934253	0.001909750	0.719959002	74.44
8	2.147132099	0.001455409	0.548676409	84.89
9	4.421040534	0.001899804	0.716209346	74.65

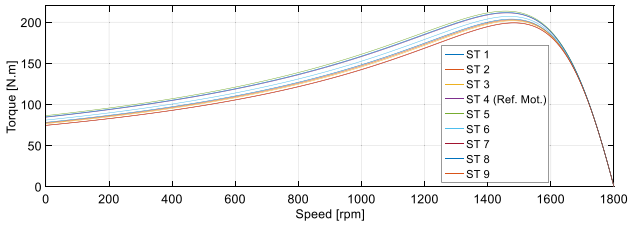

Fig. 3. Torque–speed curves for nine stator slot types.

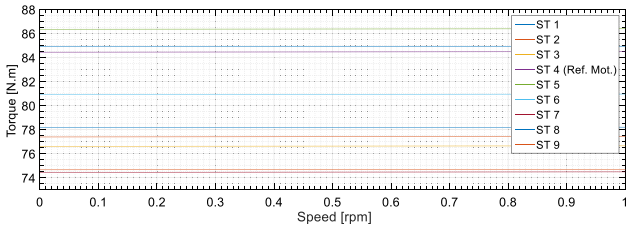

Fig. 4. Detailed figure for starting torque period.

reactance values have been calculated for each slot structure. In the last stage, torque–speed curves have been plotted for each slot structure.

IV. RESULT AND DISCUSSION

The obtained stator slot permeance coefficients, stator inductance and reactance, and starting torque results have been given in Table II for nine different slot structures.

The torque–speed curves obtained for nine different stator slot structures have been shown in Fig. 1. The change of the starting torque according to the slot structures has been shown in Fig. 3. A detailed graph of the starting torque has been shown in Fig. 4 for the number of speed for 0–1 interval.

When Fig. 4 has been examined, the nominal torque values for different slot structures are almost the same. It has been also clear that the maximum torque values also differ according to the slot structure, because of the maximum slip changes depending on the X_1 and X_2 parameters.

When the figures and tables are examined, it has been seen that there are significant differences in the starting torque values. The lowest starting torque has belonged to the slot structure numbered ST7 and the value has been obtained as 74.44 N·m. The maximum starting torque has been obtained from slot number ST5 and the value has been determined as 86.35 N·m. Using a different slot structure, it has been seen that a 16% increase in the starting torque can be achieved compared with the structure of the slot giving the best and the worst starting torque value. The starting torque of the reference motor's value has been obtained as 84.44 N·m.

V. CONCLUSION

In this paper, the slot permeance value's coefficient of nine different stator slot structures that are most used in the stator slot structures of induction motors has been examined for obtaining the best starting torque. However, inductance and reactance calculations have been performed for each slot structure. After finding the leakage reactance values, the torque–speed curves for each slot structure have been obtained and the starting torque has been performed. From the obtained results, it has been determined that the starting torque has changed in great ratio as the stator slot structure has changed. It has been shown that a 16% improvement can be achieved at the starting torque with the change in slot structure. This provides a great advantage to be able to move a heavy load.

REFERENCES

[1] R. Rinkevičienė and A. Petrovas, "Modelling of frequency controlled induction drive with ventilator type load," *Elect. Eng. Electron.*, vol. 6, no. 94, pp. 69–72, 2009.

[2] R. Hedjar, P. Boucher, and D. Dumur, "Robust nonlinear receding-horizon control of induction motors," *Int. J. Elect. Power Energy Syst.*, vol. 46, pp. 353–365, Mar. 2013.

[3] I. Martin-Diaz, D. Morinigo-Sotelo, O. Duque-Perez, R. A. Osornio-Rios, and R. J. Romero-Troncoso, "Hybrid algorithmic approach oriented to incipient rotor fault diagnosis on induction motors," *ISA Trans.*, vol. 80, pp. 427–438, Sep. 2018.

[4] L. Monjo, F. Córcoles, and J. Pedra, "Parameter estimation of squirrel-cage motors with parasitic torques in the torque–slip curve," *IET Electr. Power Appl.*, vol. 9, no. 5, pp. 377–387, May 2015.

[5] A. C. C. Wengerkievicz *et al.*, "Estimation of three-phase induction motor equivalent circuit parameters from manufacturer catalog data," *J. Microw., Optoelectron. Electromagn. Appl.*, vol. 16, no. 1, pp. 90–107, 2017.

[6] S. P. Khade, "Measurement of rotor leakage reactance of induction motor," *Int. J. Elect., Electron. Data Commun.*, vol. 1, no. 3, pp. 49–51, 2013.

[7] X. Bao, C. Di, and Y. Fang, "Analysis of slot leakage reactance of submersible motor with closed slots during starting transient operation," *J. Elect. Eng. Technol.*, vol. 11, no. 1, pp. 135–142, 2016.

[8] K. Nishihama, K. Ide, H. Mikami, T. Fujigaki, and S. Mizutani, "Starting torque analysis of cage induction motor using permeance model considering magnetic saturation by leakage flux," in *Proc. IEEE ICEMS*, Tokyo, Japan, Nov. 2009, pp. 1–6.

[9] W. Dong, W. Xin-Zhen, M. A. Wei-Ming, G. Yun-Jun, and C. Jun-Quan, "Calculation of stator leakage reactances of fifteen-phase induction motor with non-sinusoidal supply," *Proc. Chin. Soc. Elect. Eng.*, vol. 30, no. 6, pp. 41–47, 2010.

[10] Y. Li, S. Li, and B. Sarlioglu, "Analysis of pulsating torque in squirrel cage induction machines by investigating stator slot and rotor bar dimensions for traction applications," in *Proc. IEEE ECCE*, Denver, CO, USA, Sep. 2013, pp. 246–253.

[11] A. Boglietti, A. Cavagnino, and M. Lazzari, "Computational algorithms for induction-motor equivalent circuit parameter determination—Part I: Resistances and leakage reactances," *IEEE Trans. Ind. Electron.*, vol. 58, no. 9, pp. 3723–3733, Sep. 2011.

[12] S. Nandi, "Slot permeance effects on rotor slot harmonics in induction machines," in *Proc. IEEE IEMDC*, Madison, WI, USA, Jun. 2003, pp. 1633–1639.

[13] J. Staszak, "Determination of slot leakage inductance for three-phase induction motor winding using an analytical method," *Arch. Elect. Eng.*, vol. 62, no. 4, pp. 569–591, 2013.

[14] M. V. Deshpande, "Design and testing of electrical machines," in *Machines*. New Delhi, India: PHI Learning Private Limited, 2010, pp. 1–510.

[15] I. Boldea and S. A. Nasar, "The induction machines design handbook," in *Machines*. Boca Raton, FL, USA: CRC Press, 2010, pp. 1–845.

[16] Z. Ling, L. Zhou, S. Guo, and Y. Zhang, "Equivalent circuit parameters calculation of induction motor by finite element analysis," *IEEE Trans. Magn.*, vol. 50, no. 2, Feb. 2014, Art. no. 7020604.
[17] R. L. J. Sprangers, J. J. H. Paulides, K. O. Boynov, J. Waarma, and E. A. Lomonova, "Design and optimization tools for high-efficiency three-phase induction motors," in *Proc. EPE*, Lille, France, Sep. 2013, pp. 1–10.
[18] Y. Duan, "Method for design and optimization of surface mount permanent magnet machines and induction machines," Ph.D. dissertation, Dept. Elect. Comput. Eng., Georgia Inst. Technol., Atlanta, GA, USA, 2010.
[19] I. Boldea and S. A. Nasar, "The induction machine handbook," in *Machines*. Boca Raton, FL, USA: CRC Press, 2002, pp. 1–883.
[20] D. Bulgan, "A software for analysis of permanent magnet ac motors," M.S. thesis, Dept. Elect. Electron. Eng., Middle East Tech. Univ., Ankara, Turkey, 2014.
[21] J. F. Gieras, "Permanent magnet motor technology: Design and applications," in *Machines*, 3rd ed. Boca Raton, FL, USA: CRC Press, 2010, pp. 1–603.
[22] J. Pyrhonen, T. Jokinen, and V. Hrabovcova, "Design of rotating electrical machines," in *Machines*. New Delhi, India: Wiley, 2008, pp. 1–584.
[23] R. Pentiuc, G. Baluta, C. Popa, and G. Mahalu, "Calculation of reactances for ring windings to toroidal inductors of hybrid induction machine," *Adv. Elect. Comput. Eng.*, vol. 9, no. 2, pp. 70–74, 2009.

Asım Gökhan Yetgin was born in Kütahya, Turkey, in 1979. He received the B.Sc. degree from the Department of Electrical Electronics Engineering, Selcuk University, Konya, Turkey, in 2001, the M.Sc. degree from Dumlupinar University, Kutahya, Turkey, in 2004, and the Ph.D. degree from Sakarya University, Sakarya, Turkey, in 2010.

He is currently an Assistant Professor with the Department of Electrical Electronics Engineering, Mehmet Akif Ersoy University, Burdur, Turkey. His current research interests include optimization, design and modeling of electrical machines, finite-element method, and energy saving.